

# NMR Study of the Synthesis of Alkyl-Terminated Silicon Nanoparticles from the Reaction of SiCl<sub>4</sub> with the Zintl Salt, NaSi

Daniel Mayeri,<sup>†</sup> Brian L. Phillips,<sup>\*,‡</sup> Matthew P. Augustine,<sup>\*,†</sup> and Susan M. Kauzlarich<sup>\*,†</sup>

Departments of Chemistry and Chemical Engineering and Material Science,  
One Shields Ave, University of California, Davis, California 95616

Received May 23, 2000. Revised Manuscript Received December 4, 2000

The synthesis of silicon nanoclusters and their characterization by multinuclear solid-state nuclear magnetic resonance (NMR) is presented. A combination of <sup>23</sup>Na, <sup>29</sup>Si, and <sup>13</sup>C magic angle spinning with and without cross polarization to <sup>1</sup>H nuclei have been used to investigate the reaction of sodium silicide (NaSi) with silicon tetrachloride (SiCl<sub>4</sub>) followed by varying degrees of surface passivation. The <sup>23</sup>Na and <sup>29</sup>Si NMR spectra of NaSi distinguish the two crystallographically inequivalent sites for each, consistent with the crystal structure. This compound exhibits extreme diamagnetic chemical shifts for <sup>29</sup>Si of –361 and –366 ppm. NaSi is reacted with SiCl<sub>4</sub> in refluxing ethylene glycol dimethyl ether to produce both amorphous and crystalline Si nanoparticles with surfaces capped by chlorine. This reaction produces new <sup>29</sup>Si resonances that survive subsequent capping and oxidation reactions. The <sup>29</sup>Si NMR spectrum shows that the product is incompletely passivated with butyl groups and gives several peaks lying between –67 and –81 ppm that can be attributed to surface silicon atoms. Further reaction of this product with water produces a new NMR spectrum consistent with further termination of the surface by –OH groups.

## Introduction

Quantum confinement in nanostructured crystalline silicon (Si) and isolated silicon nanoclusters (*nc*-Si) is of great interest from an academic as well as an industrial applications perspective. These quantum size effects have traditionally been monitored by photoluminescence spectroscopy; however, the mechanism for spectral modifications as a function of synthetic preparation is still a controversial topic.<sup>1</sup> To address this concern, several synthetic strategies for the preparation of isolated *nc*-Si, including solution synthesis,<sup>2,3</sup> chemical vapor deposition,<sup>4</sup> gas-phase decomposition of silanes,<sup>5,6</sup> and ultrasonic dispersion of porous silicon,<sup>7</sup> have been developed. Recently, in our laboratory we accomplished an alternative solution-phase approach using reactive Zintl salts.<sup>8–15</sup> This work demonstrated

that both silicon and germanium nanoclusters with functionalized surfaces can be formed in solution at low temperatures and ambient pressures. At the heart of this approach for silicon is the reaction of a Zintl salt with silicon tetrachloride SiCl<sub>4</sub> to form chloride-capped silicon nanoclusters, *nc*-Si/Cl. Subsequent reaction of this product with either RLi or RMgCl (R = –methyl, –ethyl, –butyl, and –octyl) terminates the particles with alkyl groups forming R-capped silicon nanoclusters, *nc*-Si/R. In the modified synthesis presented here the Zintl salt NaSi has been used to produce passivated *nc*-Si via a reaction with SiCl<sub>4</sub> while butyllithium, BuLi, was used as a passivation precursor. The availability of 100% abundant <sup>23</sup>Na and <sup>29</sup>Si and <sup>13</sup>C nuclei in these compounds suggests that NMR can be used to characterize the products generated in the solution phase synthesis of organically passivated *nc*-Si.

\* To whom correspondence should be addressed.

<sup>†</sup> Department of Chemistry.

<sup>‡</sup> Department of Chemical Engineering and Material Science.

(1) Brus, L. E. In *The Robert A. Welch Foundation 39th Conference on Chemical Research, Nanophase Chemistry*, Houston, Texas, 1995; p 21.

(2) Heath, J. R. *Science* **1992**, *258*, 1131.

(3) Wilcoxon, J. P.; Samara, G. A.; Provencio, P. N. *Phys. Rev. B* **1999**, *60*, 2704.

(4) Berger, S.; Schachter, L.; Tamir, S. *Nanostruct. Mater.* **1997**, *8*, 231.

(5) Fojtik, A.; Weller, H.; Fiechter, S.; Henglein, A. *Chem. Phys. Lett.* **1987**, *134*, 477.

(6) Littau, K. A.; Szajowshki, P. J.; Muller, A. J.; Kortan, A. R.; Brus, L. E. *J. Phys. Chem.* **1993**, *97*, 1224.

(7) Bley, R. A.; Kauzlarich, S. M.; Davis, J. E.; Lee, H. W. H. *Chem. Mater.* **1996**, *8*, 1881.

(8) Bley, R. A.; Kauzlarich, S. M. *J. Am. Chem. Soc.* **1996**, *118*, 12461.

(9) Bley, R. A.; Kauzlarich, S. M. *A Low-Temperature Solution Phase Route for the Synthesis of Silicon Nanoclusters*; Kluwer Academic Publishers: Dordrecht, 1996; p 467.

(10) Bley, R. A.; Kauzlarich, S. M. In *Nanoparticles and Nanostructure Films*; Fendler, J. H., Ed.; Wiley-VCH: New York, 1998; p 101.

(11) Taylor, B. R.; Kauzlarich, S. M.; Delgado, G. R.; Lee, H. W. H. *Chem. Mater.* **1998**, *10*, 22.

(12) Taylor, B. R.; Kauzlarich, S. M.; Delgado, G. R.; Lee, H. W. H. *Chem. Mater.* **1999**, *11*, 2493.

(13) Kauzlarich, S. M.; Chan, J. Y.; Taylor, B. R. In *Inorganic Materials Synthesis: New Directions for Advanced Materials*; Winter, C. H., Hoffman, D. M., Eds.; ACS Symposium Series; American Chemical Society: Washington, DC, 1999; Vol. 727.

(14) Yang, C.-S.; Bley, R. A.; Kauzlarich, S. M.; Lee, H. W. H.; Delgado, G. R. *J. Am. Chem. Soc.* **1999**, *121*, 5191.

(15) Yang, C.-S.; Kauzlarich, S. M.; Wang, Y. C. *Chem. Mater.* **1999**, *11*, 3666.

Because the first step in this reaction involves the Zintl salt NaSi, a useful starting point for the introduction of the role of nuclear magnetic resonance (NMR) in this study is a brief review of the literature concerning this compound. The only NMR spectral data available for NaSi is reported by Gryko et al. in connection with a study of the decomposition pathways of NaSi into several clathrate compounds.<sup>16,17</sup> The solid-state MAS NMR spectra for both <sup>23</sup>Na and <sup>29</sup>Si nuclei are reported for the clathrate decomposition products. However, for NaSi only the <sup>23</sup>Na NMR spectrum is presented. This spectrum consists of one peak centered at 50 ppm with respect to the standard NaCl(aq) at 0 ppm. Although the <sup>23</sup>Na NMR appears to be quite sensitive to electronic structure (i.e., the clathrate materials displayed shifts in excess of 1000 ppm), it is of little use in the study of *nc*-Si because Na is removed from the phase of interest. <sup>29</sup>Si solid-state NMR proved to be equally informative in the study of these clathrate decomposition products because of the large paramagnetic <sup>29</sup>Si NMR chemical shifts (650 and 825 ppm with respect to the standard tetramethylsilane at 0 ppm) due to charge density on nearby Na.

The strength of <sup>29</sup>Si solid-state NMR as a structural tool has also been demonstrated in recent studies of nanostructured domains found in both porous and amorphous Si.<sup>18–22</sup> The combined use of cross polarization from <sup>1</sup>H nuclei with and without magic angle spinning (MAS) was used to identify both interior and exterior Si sites as well as to determine the level of crystallinity and degree of protonation and oxidation of the Si sites within the porous material. Observation of the signal by <sup>29</sup>Si{<sup>1</sup>H} cross polarization confirmed the existence of protons on the surface of porous Si. For amorphous Si formed by rf-sputter deposition, the correlation of crystallinity with annealing temperature was monitored with <sup>29</sup>Si MAS NMR. With regards to the study reported here on *nc*-Si, the important result for amorphous Si is that the peaks in the <sup>29</sup>Si solid-state NMR spectra are observed to be very broad but narrow as the degree of order increases with annealing. Crystalline Si gives a separate resonance, differing from amorphous Si in width and position.

The usefulness of multinuclear solid-state NMR in the studies mentioned above is exploited here to analyze the products at each step in the solution synthesis of butyl-capped silicon nanoclusters, *nc*-Si/Bu, from NaSi. Details of this synthesis appear in the next section; however, for the sake of clarity, a brief discussion is provided here. Initially, NaSi is formed from a reaction of Na metal and Si solid. Following characterization by <sup>23</sup>Na and <sup>29</sup>Si MAS NMR, NaSi was reacted with SiCl<sub>4</sub> to form a *nc*-Si/Cl sample. This powdered solid was

characterized by NMR before further reaction with BuLi. An incompletely organically passivated sample of chlorobutyl-capped silicon nanoclusters, *nc*-Si/Cl,Bu, results after a 12-h reaction with BuLi. The degree of surface passivation is confirmed by reacting the *nc*-Si/Cl,Bu sample with water. Water reacts with the chloride-capping groups and an oxidized *nc*-Si/OH sample is produced.

## Experimental Section

**Materials and Methods.** Silicon (99.99999+%) was obtained from Johnson Matthey, tetra-*n*-butylsilane was acquired from United Chemical Technologies, and ethylene glycol dimethyl ether or glyme, HPLC-grade hexane, SiCl<sub>4</sub> (99.999%), dichlorodimethylsilane (CH<sub>3</sub>)<sub>2</sub>SiCl<sub>2</sub> (99%), and *n*-BuLi were all purchased from Aldrich. Prior to use, the glyme was degassed, dried, and distilled over sodium potassium alloy but all other reagents were used as received without further purification. All sample manipulations were handled via standard inert atmosphere techniques. Glassware was silonated by reaction for 1 h with a 2% solution of (CH<sub>3</sub>)<sub>2</sub>SiCl<sub>2</sub> in toluene followed by repeated washes with hexane and methanol. Glassware was dried overnight at 120 °C and transferred hot into an N<sub>2</sub>-filled glovebox. Unless otherwise stated, all samples are air-sensitive and precautions must be taken to avoid exposure to air.

**Sodium Silicide (NaSi).** The Zintl salt NaSi was prepared by modification of a literature procedure.<sup>23</sup> In a glovebox, 500 mg of Na and 550 mg of Si were placed into a Nb tube having one end crimped and welded shut. The open end was crimped closed, transferred, and welded shut with an argon arc welder. The sealed Nb tube was sealed into a fused silica jacket under 0.25 atm of Ar gas. The Nb tube/silica jacket assembly was placed into a furnace and the temperature was raised to 650 °C at a rate of 60 °C/h. After 3 days the furnace was cooled to room temperature and the Nb tube/silica jacket assembly was transferred to a glovebox and opened. Excess solid Na was removed from the product by vacuum sublimation at 300 °C and the purified product appearing as a black microcrystalline powder was recovered. This compound was subsequently identified as NaSi by X-ray powder diffraction (Enraf Nonius Guinier camera).

**Chloride-Capped Silicon Nanoclusters (*nc*-Si/Cl).** A suspension of 400 mg of NaSi and 100 mL of dried glyme was prepared and allowed to stir and reflux under argon (Ar) gas for ≈12 h. At this point 3 mL of SiCl<sub>4</sub> was added and the suspension was allowed to reflux for another 12 h. The reaction was then allowed to cool and excess SiCl<sub>4</sub> and glyme were removed by evacuating the reaction vessel to dryness.

**Chlorobutyl-Capped Silicon Nanoclusters (*nc*-Si/Cl,Bu).** A suspension of *nc*-Si/Cl and 100 mL of dried glyme was prepared by stirring and heating. This mixture was allowed to cool to room temperature while continuing to stir and 8 mL of 2.5 M BuLi in hexane was added. This suspension was allowed to react at room temperature for ≈12 h at which time all solvent was removed by evacuating the reaction vessel. The remaining solid product corresponds to *nc*-Si/Cl,Bu and alkali chloride salts. The product was characterized by X-ray powder diffraction and FTIR. The powder diffraction pattern showed the salts and the FTIR showed the CH<sub>3</sub>– and CH<sub>2</sub>– stretches and bends.

**Oxidized Silicon Nanoclusters (*nc*-Si/OH).** The *nc*-Si/Cl,Bu containing solid was removed from the reaction vessel in an inert atmosphere momentarily exposed to air and vigorously washed with water. The resulting black powdered *nc*-Si/OH was handled in air. The black product was also characterized by X-ray powder diffraction and FTIR. No diffraction peaks were observed in the powder diffraction. The FTIR showed the Si–O stretch.

**NMR Instrumentation.** All NMR spectra were obtained with a Chemagnetics CMX-400 spectrometer using a standard

(16) Gryko, J.; McMillan, P. F.; Sankey, O. F. *Phys. Rev. B* **1996**, *54*, 3037.

(17) Gryko, J.; McMillan, P. F.; Marzke, R. F.; Dodokin, A. P.; Demkov, A. A.; Sankey, O. F. *Phys. Rev. B* **1998**, *57*, 4172.

(18) Pietrass, T.; Bifone, A.; Roth, R. D.; Koch, V. P.; Alivisatos, A. P.; Pines, A. *J. Non-Cryst. Solids* **1996**, *202*, 68.

(19) Shao, W. L.; Shinar, J.; Gernstein, B. C.; Li, F.; Lannin, J. S. *Phys. Rev. B* **1990**, *41*, 9491.

(20) Petit, D.; Chazalviel, J. N.; Ozanam, F.; Devreux, F. *Appl. Phys. Lett.* **1997**, *70*, 191.

(21) Chang, W. K.; Liao, M. Y.; Gleason, K. K. *J. Phys. Chem.* **1996**, *100*, 19653.

(22) Brandt, M. S.; Ready, S. E.; Boyce, J. B. *Appl. Phys. Lett.* **1997**, *70*, 188.

(23) Busmann, V. E. *Z. Anorg. Allg. Chem.* **1961**, *313*, 90.

Chemagnetics cross polarization MAS probe assembly configured for rotors having an outer diameter of 7.5 mm. The samples were packed into zirconium oxide rotors having O-ring sealed PTFE plugs. No significant background signal was observed for  $^{23}\text{Na}$ ,  $^{13}\text{C}$ , and  $^{29}\text{Si}$  for this configuration using the experimental conditions described below. Sample rotation rates varied from 3.2 to 6.0 kHz, depending on the experiment and the positions of principal absorption peaks. Typically, 1000–2000 acquisitions were averaged per spectrum.

All  $^{23}\text{Na}$  NMR spectra were measured under MAS at a Larmor frequency of 105.5 MHz with single-pulse excitation. Uniform excitation across the  $^{23}\text{Na}$  bandwidth was achieved by using short 1- $\mu\text{s}$  pulses where the nonselective  $\pi$  pulse length was typically 12  $\mu\text{s}$ . Relaxation delays of 1 s were sufficient to avoid signal saturation. The  $^{29}\text{Si}$  MAS and  $^1\text{H}$  decoupled  $^{29}\text{Si}$  cross polarization MAS ( $^{29}\text{Si}\{^1\text{H}\}$  CP-MAS) spectra were obtained at 79.49 MHz. Typically, pulse lengths of 6–8  $\mu\text{s}$  were used at a 31-kHz  $B_1$  field for both  $^{29}\text{Si}$  and  $^1\text{H}$  and relaxation delays were generally long enough to prevent signal saturation, usually 2 s for CP-MAS and 15–60 s for single-pulse MAS. The exception was  $\text{NaSi}$ , which exhibits an extremely long  $^{29}\text{Si}$  relaxation time for which we used a much longer relaxation delay of 500 s. The  $^{13}\text{C}\{^1\text{H}\}$  CP-MAS spectra were obtained under similar conditions at 100.63 MHz. Here, typical pulse lengths were again 6–8  $\mu\text{s}$  (31-kHz  $B_1$  field) for both  $^{13}\text{C}$  and  $^1\text{H}$  nuclei and a 5-s relaxation delay was used. Cross polarization experiments employed a ramp of the  $^1\text{H}$  rf amplitude by about  $\pm 10$  kHz to flatten the heteronuclear match condition during MAS. The cross relaxation times between  $^{29}\text{Si}$  and  $^1\text{H}$  nuclei ( $T_{\text{Si-H}}$ ) and between  $^{13}\text{C}$  and  $^1\text{H}$  nuclei ( $T_{\text{C-H}}$ ) in addition to the  $^1\text{H}$  rotating frame relaxation time ( $T_{1\rho}$ ) were measured by varying contact times from 0.1 to 20 ms. The resulting intensity variations as a function of contact time were fit to a biexponential function that assumes monoexponential  $^1\text{H}$  relaxation. Any other details of the NMR spectrometer and data processing are available upon request.

## Results and Discussion

**Sodium Silicide (NaSi).** The  $^{23}\text{Na}$  MAS NMR spectrum for  $\text{NaSi}$  is shown in Figure 1a. Two resonances are observed, each displaying fine structure due to second-order nuclear quadrupole effects. X-ray data indicate that  $\text{NaSi}$  is composed of  $\text{Si}_4^{4-}$  tetrahedra surrounded by 4  $\text{Na}^+$  cations and is monoclinic, crystallizing in the  $C2/c$  space group. There are two crystallographically inequivalent sites for both Na and Si.<sup>23</sup> Consistent with the structure for  $\text{NaSi}$ , the  $^{23}\text{Na}$  MAS center band between 20 and 60 ppm in Figure 1a is fit well with a sum of two quadrupolar powder patterns in a 1:1 intensity ratio, having an isotropic chemical shift of  $\delta_i = 56.7$  (quadrupolar coupling parameters,  $C_q = 1.25$  (5) MHz,  $\eta = 1.00$  (5)) and 49.5 ppm ( $C_q = 2.31$  (5),  $\eta = 0.15$  (5)). The quadrupolar coupling parameters and chemical shifts were obtained from simulation of the MAS central transition line shape (Figure 1a), calculated using the method of Massiot et al.<sup>24</sup> Note that the site yielding the resonance at  $\delta_i = 49.5$  ppm is most likely in a more electronically strained environment evidenced by the larger quadrupolar coupling constant  $C_q$ , but the smaller asymmetry parameter  $\eta$  suggests more axial symmetry. Other than the spinning sidebands, no other resonances are observed in the  $^{23}\text{Na}$  spectrum. Oxidation gives very strong peaks for oxide environments upfield from those due to  $\text{NaSi}$ , which allows us to use  $^{23}\text{Na}$  NMR to determine sample quality. Remeasurement of the  $^{23}\text{Na}$  NMR spectrum of the  $\text{NaSi}$

(24) Massiot, D.; Bessada, C.; Courtres, J. P.; Taulelle, F. *J. Magn. Reson.* **1990**, *90*, 231.

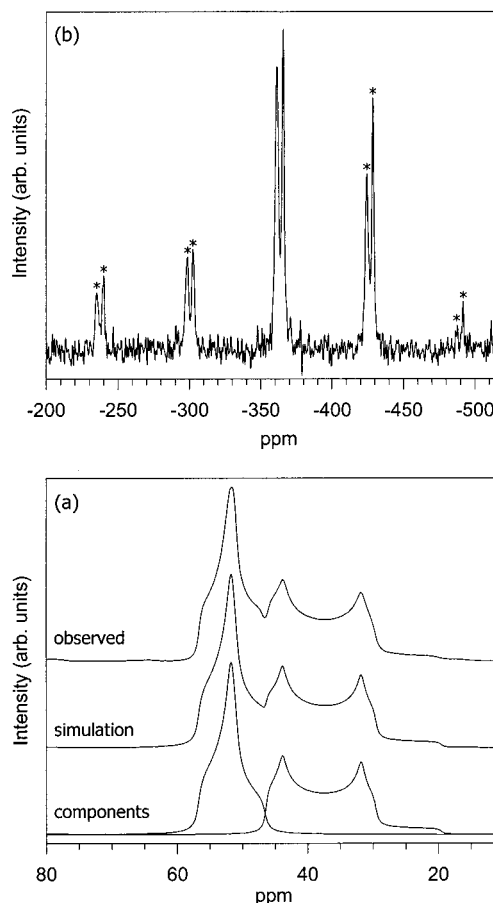


**Figure 1.** (a) The center band of the  $^{23}\text{Na}$  MAS NMR spectrum of  $\text{NaSi}$  (top) and a simulation (middle) comprising two components with approximately 1:1 intensity ratio (bottom). (b) The  $^{29}\text{Si}$  MAS NMR spectrum of  $\text{NaSi}$ . Asterisks denote spinning sidebands.

sample after several days inside the NMR probe head did not yield any new peaks, indicating that the NMR rotor is indeed sealed and the sample is isolated from the atmosphere.

The  $^{29}\text{Si}$  MAS NMR spectrum for  $\text{NaSi}$  in Figure 1b also displays two resonances, centered at  $-361.2$  (1) (a) and  $-365.5$  (1) (b) ppm with respect to tetramethylsilane (TMS) at 0 ppm. The full width at half-maximum (fwhm) of these resonances are 233 and 145 Hz, respectively. The intensity of the spinning sidebands suggests large chemical shift anisotropies for both  $^{29}\text{Si}$  sites ( $\Delta\delta_a = 214$  (3) ppm,  $\eta_a = 0.28$  (6);  $\Delta\delta_b = 236$  (3) ppm,  $\eta_b = 0.29$  (6))<sup>25,26</sup> and the far upfield shift results from the donation of electrons from the electropositive Na to the electronegative Si,<sup>27,28</sup> as is common in Zintl salts. This is different from the clathrates, which exhibit Knight shifts.<sup>29,30</sup> The spectrum in Figure 1b is the first

(25) The principal components of the chemical shift tensors were obtained from a least-squares Herzfeld-Berger analysis of the spinning sideband intensities,<sup>26</sup> using the HBA program (HBA 1.2, K. Eichele, R. E. Wasylshen, Dalhousie University).

(26) Herzfeld, J.; Berger, A. E. *J. Chem. Phys.* **1980**, *73*, 6021.

(27) Yang, L. H.; Consorte, C. D.; Fong, C. Y.; Pask, J. E.; Nabighian, E.; Kauzlarich, S. M.; Nelson, J. S. *Chem. Mater.* **1998**, *10*, 4025.

(28) Tegze, M.; Hafner, J. *Phys. Rev. B* **1989**, *40*, 9841.

(29) Shimizu, F.; Maniwa, Y.; Kume, K.; Kawaji, H.; Yamanaka, S.; Ishikawa, M. *Synth. Met.* **1997**, *86*, 2141.

(30) Ranachandran, G. K.; McMillan, P. F.; Diefenbacher, J.; Grydo, J.; Dong, J.; Sankey, O. F. *Phys. Rev. B* **1999**, *60*, 12294.

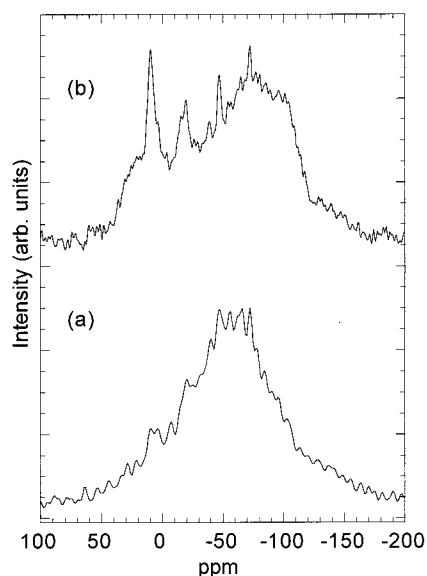


**Figure 2.** (a) The  $^{29}\text{Si}$  MAS NMR spectrum of *nc*-Si/Cl (chloride-capped silicon nanoclusters). (b) The  $^{29}\text{Si}$  CP-MAS NMR spectrum of *nc*-Si/Cl, 10-ms contact time.

reported  $^{29}\text{Si}$  NMR data for the Zintl salt NaSi and one would expect that similar phases will exhibit similarly extreme diamagnetic chemical shifts.<sup>31</sup>

**Chloride-Capped Silicon Nanoclusters (*nc*-Si/Cl).** The  $^{23}\text{Na}$  NMR spectrum of the *nc*-Si/Cl product formed from reaction of NaSi with  $\text{SiCl}_4$  displays a strong peak at 7 ppm due to the formation of sodium chloride, NaCl, in the course of reaction. Additionally, there is a weak signal from leftover unreacted NaSi, but it is 100 times less intense than the resonance for NaCl. The presence of any NaSi is surprising since the  $\text{SiCl}_4$  is in excess; however, the incomplete reaction may be due to the large scale of this reaction as compared to those of previously reported syntheses.<sup>8–10,14</sup>

Previous work on the production of *nc*-Si/Cl suggests that solution-phase synthesis generates a broad size distribution of *nc*-Si.<sup>7–10,14</sup> The  $^{29}\text{Si}$  MAS NMR spectrum of *nc*-Si/Cl is shown in Figure 2a and contains a broad peak centered at  $-55$  ppm with  $\text{fwhm} = 85.6$  ppm. The breadth and position of the peak are similar to those reported for elemental amorphous silicon.<sup>19</sup> There is no evidence for oxide environments that would yield signals between  $-90$  and  $-110$  ppm with respect to TMS at 0 ppm.<sup>32</sup> The  $^{29}\text{Si}$  NMR spectrum did not show any signs of NaSi presumably because it is below the detection limit of the NMR instrument. However, a small peak consistent with the presence of clathrate is observed at  $+700$  ppm. Additionally, no signal is observed that can be attributed to crystalline silicon, which would give a narrow peak (1–5 ppm  $\text{fwhm}$ ) near  $-80$  ppm.

Nanocrystalline and amorphous Si cannot be distinguished based solely on the NMR data. Both *nc*-Si and amorphous Si have short-range order, but can give broad  $^{29}\text{Si}$  NMR signals. Structural disorder, either in bulk material or due to a large fraction of near-surface sites, can be expected to produce a large range of

chemical shifts due to the sensitivity of the charge-transfer distribution on structural fluctuations.<sup>19,33</sup> Therefore, even if the core of the *nc*-Si particle is crystalline, strain, structural defects, and near-surface sites can all contribute to yield a range of chemical shifts. One would expect on the basis of this argument that *nc*-Si would have a broad  $^{29}\text{Si}$  NMR peak similar to that seen for amorphous Si. This prediction is further complicated due to the wide range of *nc*-Si sizes produced by these preparations and the dependence of the band gap on particle size. High-resolution electron microscopy and selected area electron diffraction provides evidence for silicon nanoclusters resulting from this synthetic method;<sup>8</sup> however, no X-ray diffraction is observed. This suggests that the sample is a mixture of small nanocrystalline particles along with larger amorphous silicon nanoparticles, both contributing to the broad  $^{29}\text{Si}$  NMR peaks.

To obtain a clearer picture of the surface sites in the *nc*-Si/Cl sample and further distinguish the spectrum of the desired products from impurities,  $^{29}\text{Si}\{^1\text{H}\}$  CP-MAS NMR was used. In this experiment, magnetization is transferred from  $^1\text{H}$  nuclei to the Si nanoparticle. Because the only significant source of H in the synthesis is the solvent, observation of the CP-MAS signal from this product indicates some reaction with solvent has occurred. The resultant  $^{29}\text{Si}$  NMR spectrum with  $^1\text{H}$  decoupling is shown in Figure 2b and clearly contains a broad peak similar in breadth to the MAS spectrum in Figure 2a. Additionally, there are several narrower peaks near 10,  $-18$ ,  $-47$ , and  $-72$  ppm. The broad component appears asymmetrical in comparison to the MAS spectrum, suggesting that the protonated Si sites have a greater chemical shift than unprotonated bulk Si. With variation of the CP contact time, both  $T_{\text{Si-H}}$  and  $T_{1\rho,\text{H}}$  near the center of the broad component centered at  $-55$  ppm can be determined as 1.7 ms and  $60 \pm 20$  ms, respectively. A comparison of Figure 2b to Figure 2a shows that in addition to the broad peak at  $-55$  ppm the narrow peaks at 10,  $-18$ ,  $-47$ , and  $-72$  ppm may also be present, but at low intensity. Since  $^1\text{H}$ - $^{29}\text{Si}$  CP-MAS increases only those spectral components reflecting  $^{29}\text{Si}$  nuclei in close proximity to  $^1\text{H}$  nuclei, and judging from the low intensity of the other narrow peaks in Figure 2b, one can assume that these peaks represent only a small fraction of the Si environments. We tentatively assign the narrow peaks at 10,  $-18$ ,  $-47$ , and  $-72$  ppm in Figure 2b to the formation of unidentified molecular species, but the present data cannot rule out the possibility that some might arise from minor protonated surface species.

The  $^{13}\text{C}\{^1\text{H}\}$  CP-MAS and  $^1\text{H}$  NMR spectra of the reaction product provide further evidence for the formation of small molecular species in this reaction. Although the spectra are not shown here, on the basis of  $^{13}\text{C}$  chemical shifts one can clearly assign peaks to residual glyme solvent molecules as well as other low intensity peaks that most likely correspond to molecular species sorbed to the surface.

**Chlorobutyl-Capped Silicon Nanoclusters (*nc*-Si/Cl,Bu).** The  $^{23}\text{Na}$  MAS NMR spectrum of *nc*-Si/Cl,Bu is virtually identical to that of the *nc*-Si/Cl

(31) Kintzinger, J. P.; Marsmann, H. In *NMR 17 Basic Principles and Progress*; Diehl, P., Fluck, E., Kosfeld, R., Eds.; Springer-Verlag: New York, 1981.

(32) Engelhardt, G.; Michel, D. *High-Resolution Solid State NMR of Silicates and Zeolites*; John Wiley: New York, 1987.

(33) Reichardt, J.; Johnson, R. H.; Ley, L. *Physica B* **1983**, *117*, 877.

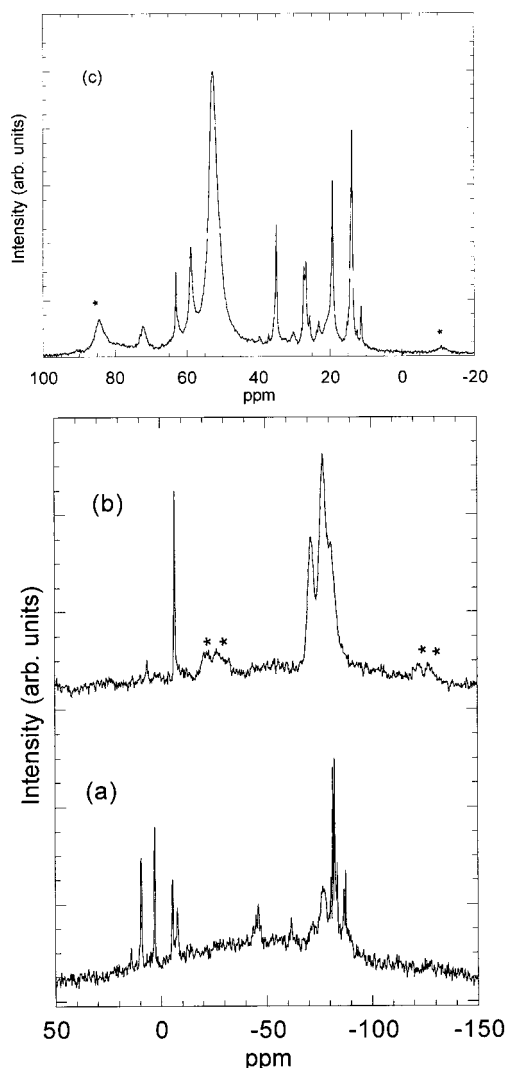


**Figure 3.** (a) The  $^{29}\text{Si}$  MAS NMR spectrum of  $nc\text{-Si/Cl,Bu}$  (butyl- and chloride-capped silicon nanoclusters). (b) The  $^{29}\text{Si}$  CP-MAS NMR spectrum of  $nc\text{-Si/Cl,Bu}$  (3-ms contact time). (c) The  $^{13}\text{C}$  CP-MAS NMR of  $nc\text{-Si/Cl,Bu}$  (5-ms contact time).

precursor, indicating the presence of  $\text{NaCl}$  with small amounts of  $\text{NaSi}$  (<1%). The  $^{29}\text{Si}$  MAS spectrum of this sample (Figure 3a) displays several new features in comparison to similar spectra in Figures 1b and 2b for the precursor compounds but also contains the broad (100 ppm fwhm) resonance centered at  $-55$  ppm. The narrow (0.2 ppm fwhm) peaks lying in the ranges from  $+10$  to  $-10$  ppm, from  $-43.6$  to  $-47.2$  ppm, from  $-80.6$  to  $-83.4$  ppm, from  $-86.6$  to  $-87.5$  ppm, and at  $-61.7$  ppm are probably due to either chlorinated polysilanes or other mobile, molecular species. More interestingly, the two broader peaks having a fwhm of 3 ppm and centered at  $-71$  and  $-77$  ppm in Figure 3a are not present in any of the precursor  $^{29}\text{Si}$  MAS NMR spectra. These peaks also occur in the  $^{29}\text{Si}\{^1\text{H}\}$  CP-MAS spectrum shown in Figure 3b, whereas most of the narrow peaks are either attenuated or removed by CP. In addition, a peak centered at  $-81.4$  ppm is amplified by CP to  $^1\text{H}$  nuclei that probably underlies the group of narrow peaks at  $-80.6$  to  $-83.4$  ppm in the MAS spectrum. The uniqueness of these three peaks centered at  $-71$ ,  $-77$ , and  $-81.4$  ppm combined with their amplification over other peaks due to CP to  $^1\text{H}$  nuclei prompts the tentative assignment of these resonances

to surface  $^{29}\text{Si}$  sites bonded to the butyl-capping groups.<sup>31,34</sup> We should note that none of the groups of narrow peaks in the MAS spectrum collapse upon application of high-power proton decoupling.

This assignment was tested in three different ways. Two of these approaches will be discussed in subsequent sections while the first method described here involves a comparison of the rotating frame relaxation time for  $^1\text{H}$  nuclei,  $T_{1\rho,\text{H}}$ , during cross polarization to both  $^{29}\text{Si}$  and  $^{13}\text{C}$  nuclei. The  $^{13}\text{C}\{^1\text{H}\}$  CP-MAS spectrum of the  $nc\text{-Si/Cl,Bu}$  sample is shown in Figure 3c. The prominent feature is a broad peak and its spinning sidebands centered at  $+53$  ppm, although several other peaks are present. These narrow peaks indicate that different types of carbon are in the sample, probably due to molecular byproducts such as alkyl silanes or chlorides or as sorbed species on the surface. The  $^{13}\text{C}$  peaks for glyme are  $+72$  and  $+59$  ppm and are present in the spectrum. The chemical shift of the broad peak is consistent with methylene carbon. However, it is impossible solely on the basis of shift to assign whether this peak is due to the methylene group bonded directly to the  $nc\text{-Si}$  surface. The rather large spinning sidebands of this peak in comparison to the other peaks in Figure 3c reflect restricted molecular motions consistent with assignment to alkyl chains bonded to surface Si atoms. Also, variation in chemical shift along the chain with distance from the Si-C bond would be expected to produce a broad peak as observed. Variable contact time  $^{13}\text{C}\{^1\text{H}\}$  CP-MAS measurements demonstrate that the protons attached to the  $^{13}\text{C}$  nucleus responsible for the peak at  $+53$  ppm have  $T_{1\rho,\text{H}} = 19$  ms. Similar variable contact time  $^{29}\text{Si}\{^1\text{H}\}$  CP-MAS measurements for the  $^{29}\text{Si}$  peaks at  $-71$ ,  $-77$ , and  $-81.4$  ppm give  $T_{1\rho,\text{H}} = 14$ , 16, and 15 ms, respectively. The similarity of  $T_{1\rho,\text{H}}$  values determined by both  $^{29}\text{Si}$  and  $^{13}\text{C}$  NMR spectroscopy suggests that these nuclei are coupled to the same  $^1\text{H}$  spin reservoir and thus likely lie in close proximity to each other. The sensitivity of this type of comparison is clearly seen in the much different  $T_{1\rho,\text{H}}$  value of 5.4 ms observed for the peak at  $+72$  ppm in Figure 3c and 60 ms for the broad  $^{29}\text{Si}$  component. Although this exercise suggests that surface Si sites can be indirectly identified solely by NMR, no direct proof is evident in any of these measurements. The only way to unequivocally distinguish these sites as being due to methylene carbons bonded to  $nc\text{-Si}$  is to perform a  $^{13}\text{C}\text{-}^{29}\text{Si}$  spin exchange experiment designed to measure either the  $^{13}\text{C}\text{-}^{29}\text{Si}$  through bond J or through space dipolar coupling. Such experiments require a large  $^{13}\text{C}$  magnetization either through  $^{13}\text{C}\{^1\text{H}\}$  CP or isotropic enrichment, which were not obtained for the present samples.

**Oxide-Capped Silicon Nanoclusters ( $nc\text{-Si/OH}$ ).** Exposure of  $nc\text{-Si/Cl,Bu}$  to water results in replacement of the peaks assigned to surface species with new resonances corresponding to oxide environments, supporting the previous assignments. The  $^{29}\text{Si}$  MAS spectrum for the  $nc\text{-Si/OH}$  sample shown in Figure 4a displays the broad peak at  $-55$  ppm corresponding to interior Si atoms and the collection of narrow peaks due to mixed molecular species. But whereas new peaks occur between  $-90$  and  $-110$  ppm, the peaks at  $-71$

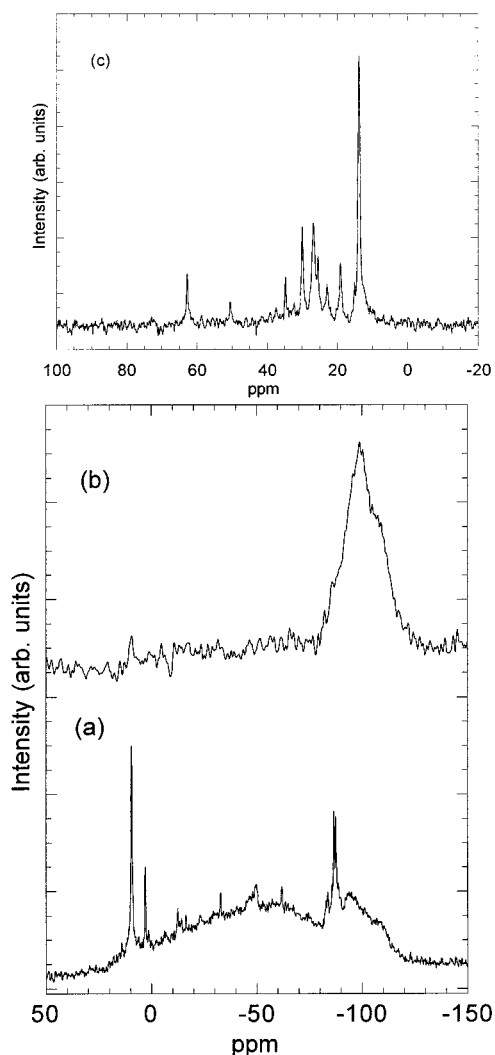


**Figure 4.** (a) The  $^{29}\text{Si}$  MAS NMR spectrum of *nc*-Si/OH (oxide-capped silicon nanoclusters). (b) The  $^{29}\text{Si}$  CP-MAS NMR spectrum of *nc*-Si/OH (3-ms contact time). (c) The  $^{13}\text{C}$  CP-MAS NMR spectrum of *nc*-Si/OH (5-ms contact time).

and  $-77$  ppm are no longer present. The  $^{29}\text{Si}\{^1\text{H}\}$  CP-MAS NMR spectrum in Figure 4b shows a set of overlapping peaks near  $-100$  ppm superimposed on a very broad peak ( $>100$  ppm fwhm) centered near  $-80(\pm 10)$  ppm. The feature near  $-100$  ppm is fit well with a sum of three Gaussian curves centered at  $-89$ ,  $-98$ , and  $-107$  ppm (each 10 ppm fwhm). With reference to the literature, one finds that oxidized Si typically displays  $^{29}\text{Si}$  NMR shifts between  $-85$  and  $-110$  ppm.<sup>32</sup> These new peaks in the CP-MAS spectrum are consistent with the presence of hydroxyl groups on the surface of the nanocluster. To be more precise, geminal silanol,

single hydroxyl silanol, and internal oxides in silica gels display  $^{29}\text{Si}$  shifts of  $-89$ ,  $-98$ , and  $-107$  ppm, respectively.<sup>35</sup> Consistent with the  $^{29}\text{Si}$  MAS spectrum in Figures 4a and 4b, the  $^{13}\text{C}\{^1\text{H}\}$  CP-MAS spectrum in Figure 4c lacks the peak at  $+53$  ppm assigned to the methylene C in the butyl-capping group. Additionally, there is no evidence for resonances due to residual glyme.

The loss of the  $^{29}\text{Si}$  peaks centered at  $-71$ ,  $-77$ , and  $-81.4$  ppm and the  $^{13}\text{C}$  peak centered at the  $+53$  ppm spectrum along with the addition of  $^{29}\text{Si}$  peaks at  $-100$  and  $-110$  ppm by reacting *nc*-Si/Cl,Bu with water to form *nc*-Si/OH suggest that hydroxyl groups have replaced terminating butyl groups. The loss of butyl groups in this reaction and the appearance of hydroxyl groups implies that the surface silicon sites are not completely passivated by butyl groups in the *nc*-Si/Cl,Bu sample, an observation consistent with the presence of chlorides on the nanocrystal surface.

### Summary

The surface termination of Si nanoclusters produced by reaction of the Zintl salt, NaSi, with  $\text{SiCl}_4$  has been investigated. The spectra show that there are side reactions that provide low yields of molecular impurities that contribute to the complexity of the NMR spectra. These molecular impurities provide narrow peaks that can easily be identified and disregarded in the analysis of the surface termination of the Si nanoclusters. The samples studied are a mixture of nanocrystalline and amorphous Si nanoclusters. Interpretation of the primary peaks in the NMR is consistent with alkyl termination of the Si nanoclusters. Oxidation of the partially terminated surface removes spectral components associated with the butyl-capping groups, supporting the peak assignments. This study provides the first direct evidence for the surface termination of these nanoclusters. Further work on size-selected nanoclusters is in progress and will provide more information concerning the surface derivitization and quantum confinement effects.

**Acknowledgment.** This work was funded by NSF (9803074), by the Petroleum Research Foundation administered by the ACS, and by the Campus Laboratory Collaborations Program of the University of California. Work was performed under the auspices of the U.S. Department of Energy by Lawrence Livermore National Laboratory under Contract W-7405-Eng-48.

CM000418W

(35) Maciel, G. E.; Sindorf, D. U. *J. Am. Chem. Soc.* **1980**, *102*, 7606.